Linear Phase Tuning of Spin Torque Oscillators Using In-Plane Microwave Fields

Tui Zeng[1], Yan Zhou[2], Johan Åkerman[3,4], P. T. Lai[1], and Philip W. T. Pong[1]

[1]Department of Electrical and Electronic Engineering, The University of Hong Kong, Hong Kong
[2]Department of Physics, The University of Hong Kong, Hong Kong
[3]Materials Physics, School of Information and Communication Technology, KTH Royal Institute of Technology, 164 40 Kista, Sweden
[4]Department of Physics, University of Gothenburg, 412 96 Gothenburg, Sweden

We demonstrate numerically and analytically that a nano-pillar spin torque oscillator (STO), operating either with in-plane or out-of-plane free-layer precession, locks to a microwave field (H_{ac}) having the same frequency as the STO. By varying the spatial direction of the microwave field, we further show the preferred phase shift ($\Delta\Phi_0$) between the STO and H_{ac} can be tuned in a linear fashion. We explain this phenomenon by using a magnetic-energy-based analysis. Our results provide a way to synchronize serially connected STOs by tuning the phase shift of each individual STO with external microwave field, which may enhance the locking efficiency, the locking range, and the output power of the serially connected STOs.

***Index Terms*—Locking frequency, microwave field, phase lock, spin torque oscillator.**

I. Introduction

THE spin transfer torque phenomenon firstly predicted by Slonczewski and Berger has inspired a large number of theoretical and experimental studies in the last decade [1]–[8]. A spin-torque-oscillator (STO) is a nanosized device driven by spin-polarized direct current. It holds great promise for telecommunication applications thanks to its capability of ultra-wide frequency-range microwave signal generation from around 100 MHz to above 60 GHz and its ability to be easily modulated at very high frequencies. The practical utilization of STOs as radio-frequency and microwave sources has been hampered by their limited output power and poor signal quality. After it was experimentally shown that STOs can phase lock to an external microwave signal, the concept of serially connected STOs was proposed. The serially connected STOs can be mutually synchronized by sharing their self-generated microwave signals [9], leading to both higher output powers and improved signal quality. These original studies were followed by a number of subsequent studies [10], [11]; however, they have all focused their attention on phase locking and mutual synchronization due to microwave current alone.

In this work, we present a macrospin study of how STOs lock to microwave field. By adjusting the direction of the applied microwave field, we demonstrate that we can linearly tune the preferred phase shift $\Delta\Phi_0$ between the STO and the microwave field from 0° to 180°, which offers an approach for enhancing the locking efficiency and the locking range of serially connected STOs. This can improve the output power and signal quality of the STOs.

II. Numerical Details

A typical giant magnetoresistance trilayer [12] consisting of a fixed ferromagnetic layer, a free ferromagnetic layer, and a nonmagnetic spacer layer is considered in our macrospin approximation and shown in Fig. 1(a). The time evolution of the free-layer magnetization $\boldsymbol{m}$ [13] [Fig. 1(b)] is found using the Landau-Lifshitz-Gilbert-Slonczewski equation [1], [2]

$$\frac{d\hat{m}}{dt} = -|\gamma|\hat{m}\times H_{eff} + \alpha\hat{m}\times\frac{d\hat{m}}{dt} + |\gamma|\frac{\eta I_{dc}}{2\mu_0 M_s e V_f}\hat{m}\times(\hat{m}\times\hat{M}) \quad (1)$$

where $\boldsymbol{m}$ and $\boldsymbol{M}$ are the unit vectors along the magnetization of the free layer and fixed layer respectively, γ is the gyromagnetic ratio, α is the damping coefficient, μ_0 is the magnetic vacuum permeability, η is the spin transfer efficiency, M_s is the free-layer saturation magnetization, and V_f is the volume of the free layer. The microwave field H_{ac}, which is the external driving force for tuning the preferred phase shift $\Delta\Phi_0$, is applied in the x-y film plane forming an angle β with respect to the easy (x) axis. A dc field H_{dc} is also applied along the easy axis. The effect of the demagnetization tensor is separated into a positive anisotropy field (H_k) along x and a negative out-of-plane demagnetizing field (H_d). We obtain the effective field as

$$H_{eff} = (H_{dc} + H_{ac}\cos\beta)\hat{e}_x + H_k(\hat{m}\cdot\hat{e}_x)\hat{e}_x + H_{ac}\sin\beta\hat{e}_y - H_d(\hat{m}\cdot\hat{e}_z)\hat{e}_z \quad (2)$$

where $\hat{e}_x$, $\hat{e}_y$, and $\hat{e}_z$ are the unit vectors along x (in-plane easy axis), y, and z (out-of-plane), respectively. In this study, the free layer is composed of a typical Co thin film with its lateral dimension defined as an elliptical shape of 130 × 70 nm^2 and thickness 3 nm. The values of some other parameters used in the calculations are as follows [14]: $|\gamma| = 1.76\times 10^{11}$ Hz/T, $\eta = 0.35$, $M_s = 1270$ kA/m, $\alpha = 0.007$, $H_{dc} = 0.2$ T, $H_d = 1.6$ T, and $H_k = 0.05$ T.

Before applying any external microwave field to the device, the relation between STO precessional behavior f and direct current I_{dc} is explored (Fig. 2). When I_{dc} is smaller than the critical current I_c (2.8 mA here), the free-layer magnetization remains in a static state. When I_{dc} increases beyond the critical current, the free-layer magnetization starts to precess around

Manuscript received April 29, 2013; revised July 30, 2013; accepted August 01, 2013. Date of current version December 23, 2013. Corresponding author: P. W. T. Pong (e-mail: ppong@eee.hku.hk).

Color versions of one or more of the figures in this paper are available online at http://ieeexplore.ieee.org.

Digital Object Identifier 10.1109/TMAG.2013.2276665

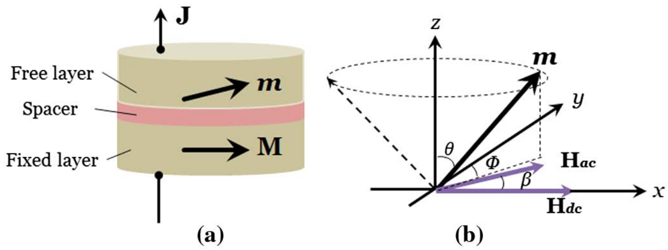

Fig. 1. Schematic illustration of the spin torque oscillator. (a) Device structure. (b) Free-layer magnetization vector in spherical coordinates.

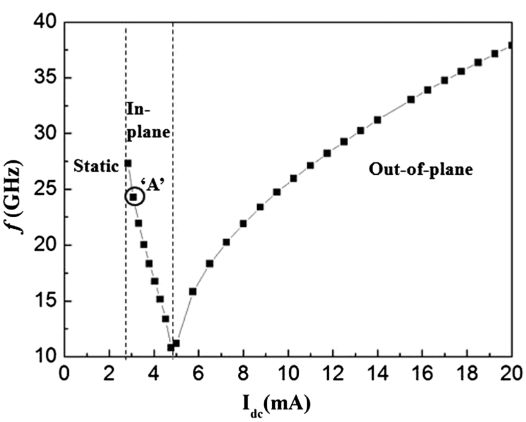

Fig. 2. STO precessional behavior under direct current: oscillation frequency f vs I_{dc}.

the easy axis (x-axis) which we describe as in-plane precession. In this regime, as I_{dc} increases, the precessional frequency decreases. When I_{dc} further increases, the free-layer magnetization begins to precess around an equilibrium angle pointing out-of-plane, and the precessional frequency starts to increase with I_{dc} [15], [16]. This V-shaped current-frequency relation coincides with the former investigation [17].

After having determined the I_{dc}-f curve, the external in-plane microwave field is applied. To avoid any frequency pulling or pushing induced by the applied field, we set the frequency of H_{ac} to that of the intrinsic precession of the STO. The amplitude of the H_{ac} is as large as 1% of the H_{dc}. Hence, the microwave field H_{ac} can be expressed as $H_{ac} = 0.002 \times \sin[2\pi \times f(I_{dc}) \times t]$, where $f(I_{dc})$ denotes the STO processional frequency under certain sweep current I_{dc}.

The manner in which the STO adjusts itself to the external microwave field H_{ac} is presented in Fig. 3 for $I_{dc} = 3$ mA (point "A" in Fig. 2) and $\beta = 0°$. The resistance of the STO is defined as

$$R_{STO} = \frac{R_{AP} + R_P}{2} - \frac{R_{AP} - R_P}{2} \cos\theta \tag{3}$$

where θ is the angle formed between the free-layer magnetization and the fixed-layer magnetization. When $\theta = 0°$ or $180°$, a parallel alignment R_P or an anti-parallel alignment R_{AP} is obtained, respectively. The free-layer magnetic energy is introduced as

$$E = -H_{dc}\cos\theta - H_{ac}(\cos\theta \cdot \cos\beta + \sin\theta \cdot \sin\phi \cdot \sin\beta) + H_k\frac{\sin^2\theta}{2} + H_d\frac{\sin^2\theta \cdot \cos^2\theta}{2} \tag{4}$$

where the first and second term represent the external field energy, the third term represents the anisotropy field energy, and the fourth term represents the demagnetization field energy.

Before the microwave field is applied, the STO is in a free running state characterized by stable precession of the free-layer magnetization and a constant magnetic energy [area I in Fig. 3(a) and Fig. 3(b)]. When the microwave field is applied, the STO first experiences a transient stage. During this regime, periodic precession is still sustained while the average resistance and average magnetic energy in each period has changed, as shown in area II in Fig. 3(a) and Fig. 3(c). Meanwhile, the STO is adjusting itself to the ac field, and the phase shift $\Delta\Phi$ between the oscillator and the ac field evolves to a final preferred value $\Delta\Phi_0$. After the transient stage, a new magnetization oscillator orbit is formed, as shown in area III in Fig. 3(a) and Fig. 3(d).

We now proceed to show the tuning of the phase shift $\Delta\Phi$ through varying the direction of the microwave field. This is carried out by changing the in-plane angle β from 0° to 180°. The preferred phase shift $\Delta\Phi_0$ is determined during the stable stage for angles $\beta = 0°, 30°, 60°, 90°, 120°, 150°$, and $180°$. As shown in Fig. 4(a), when I_{dc} is below the critical value, the STO is under static state and no preferred phase shift is formed. As I_{dc} increases, the STO enters its in-plane precession state. It is observed that when $0° \le \beta < 90°$, the phase shift stays around 0° which indicates perfect synchronization. When $\beta = 90°$, the phase shift turns to 90° [18]. Finally, when $90° < \beta \le 180°$, the phase shift value becomes 180°. Fig. 4(b) demonstrates the phase shift measurement of point "p" in Fig. 4(a). A phase hopping occurs as shown in Fig. 4(c). To further verify this phase hopping, the phase shifts for $\beta = 89°$ and $\beta = 91°$ are calculated and this hopping phenomenon is also observed. When I_{dc} is further increased to drive the STO into its out-of-plane precession state, this discretized behavior is replaced by an entirely linear relation, $\Delta\Phi = 180°$-β, as shown in Fig. 4(d).

To explain the in-plane phase hopping and the out-of-plane linear phase adjusting phenomena analytically, we utilize a magnetic-energy-based analysis. It is important to realize that at constant direct current, the magnetic energy $E(t)$ calculated in Fig. 3 sustains a stable precession along a fixed orbit that we describe as $\zeta(I_{dc})$ [13]. The energy balance is calculated with

$$\delta E = \oint_{\zeta(I_{dc})} dE = \oint_{\zeta(I_{dc})} \left[\frac{\eta I_{dc}}{2\mu_0 M_s e V_f}\hat{m} \times \hat{M} - \alpha(\hat{m} \times H_{eff})\right] d\hat{m} \tag{5}$$

and it should be zero [19], [20] for a steady orbit such as the free running stage in Fig. 3(a). When the microwave field is applied to the STO in the transient stage, the precession orbit changes to $\zeta(I_{dc} + H_{ac})$ which directly leads to a nonzero δE. However, if the phase shift between the H_{ac} and the STO coincides with the preferred phase shift, the δE would return to zero again and run into the stable stage as shown in Fig. 3(a). Hence the evaluation of δE as a function of the relative phase $\Delta\Phi$ between H_{ac} and resistance becomes the criteria for determining the preferred phase shift.

As shown in Figs. 5 and 6, the energy balance is calculated when $I_{dc} = 3$ mA for in-plane mode and $I_{dc} = 10$ mA for out-of-plane mode under various $\Delta\Phi$. For the in-plane mode in

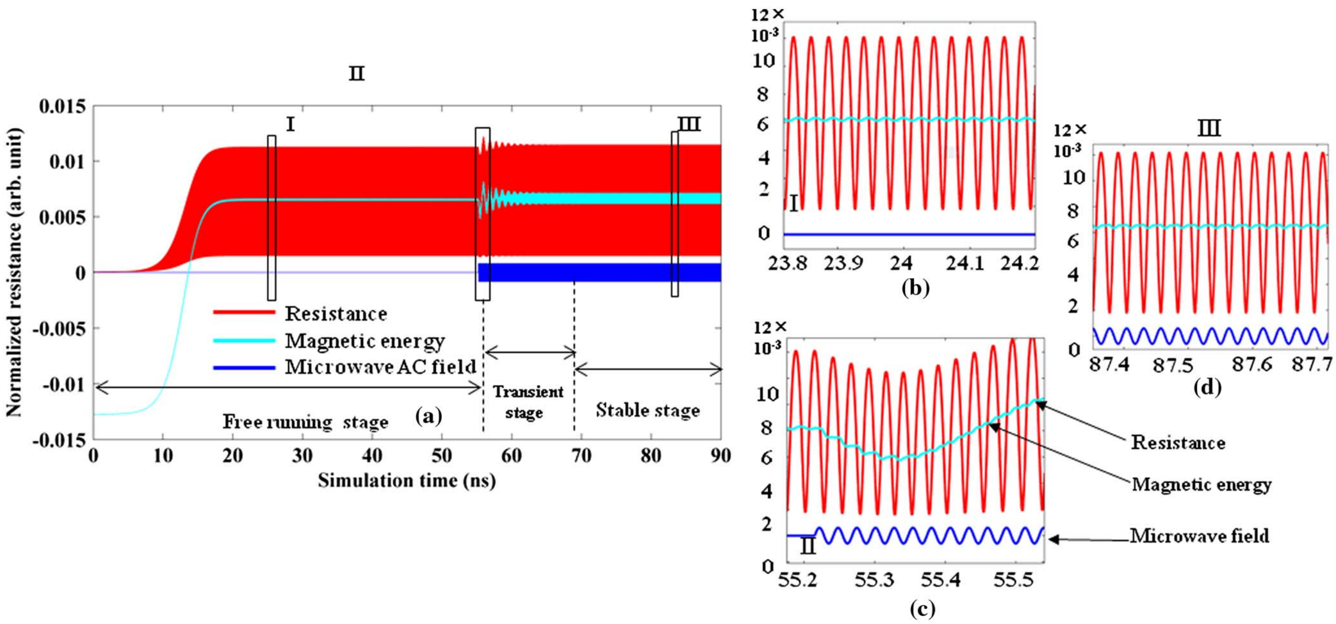

Fig. 3. (color online) (a) STO precessional behavior (resistance, magnetic energy, microwave ac field) under different direct current. (b) An amplification of area I in the free running stage of the STO. (c) An amplification of area II in the transient stage of the STO. (d) An amplification of area III in the stable stage of the STO.

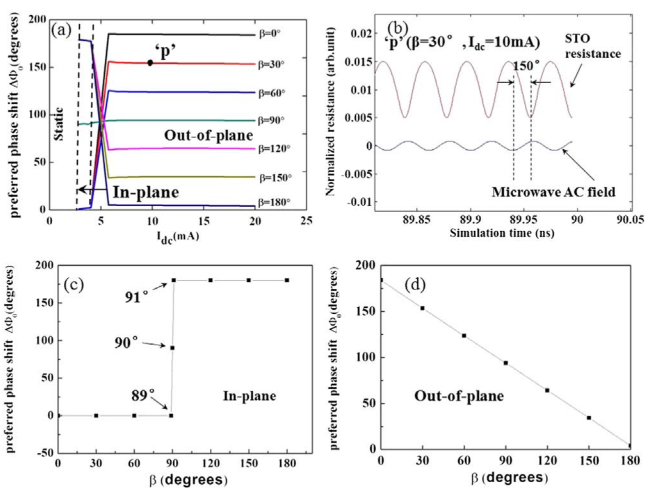

Fig. 4. (color online) (a) STO preferred phase shift $\Delta\Phi_0$ versus the dc current I_{dc} under different β values. (b) Phase shift $\Delta\Phi$ between microwave ac field and STO resistance under 10 mA dc current and 30° β angle [point "p" in Fig. 4(a)]. (c) STO preferred phase shift $\Delta\Phi_0$ versus β for in-plane mode. (d) STO preferred phase shift $\Delta\Phi_0$ versus β for out-of-plane mode.

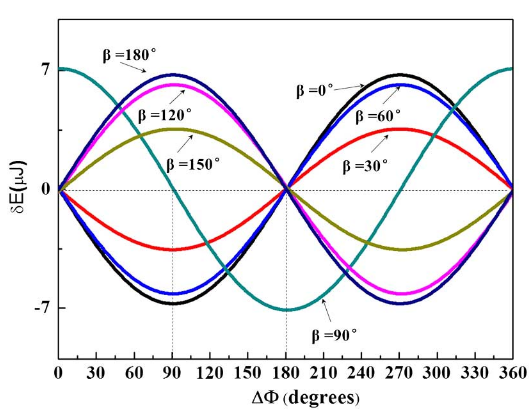

Fig. 5. (color online) Energy difference per cycle (δE) versus relative phase ($\Delta\Phi$) between the STO and the microwave field at various β when $I_{dc} = 3$ mA where the free layer of the STO is in in-plane mode.

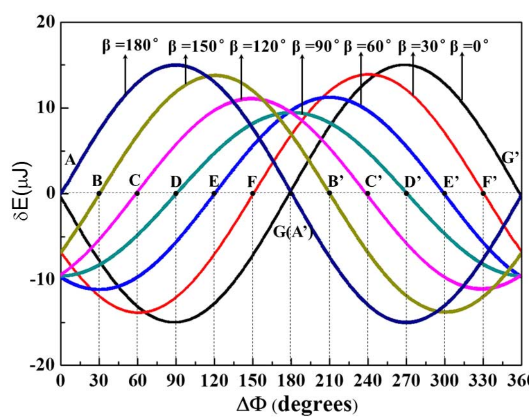

Fig. 6. (color online) Energy difference per cycle (δE) versus relative phase ($\Delta\Phi$) between the STO and the microwave field at various β when I_{dc} = 10 mA where the free layer of the STO is in out-of-plane mode.

Fig. 5, the new possible orbits are the points where $\delta E = 0$. For $0° \leq \beta < 90°$ and $90° < \beta \leq 180°$, the two possible preferred phase shifts are 0° and 180°, respectively. For $\beta = 90°$, the two possible preferred phase shifts are 90° and 270°, respectively. However, only one of them represents a stable orbit ($\Delta\Phi_0$) whereas the other orbit ($\Delta{\Phi_0}^*$) is inherently unstable.

The thermal energy (or magnetic field noise), which is regarded as an external perturbation, drives $\Delta\Phi$ away from the stable orbit point $\delta E = 0$. This leads to a change in the magnetic energy E and further results in a change of the precessional frequency f. The frequency slows down whenever the STO is ahead of the ac field and speeds up whenever it is behind. A stable orbit is always characterized by the stability criterion [17]

$$\left.\frac{\partial f}{\partial \Delta\Phi}\right|_{\Delta\Phi_0} = \left.\frac{\partial f}{\partial \delta E}\frac{\partial \delta E}{\partial \Delta\Phi}\right|_{\Delta\Phi_0} = 0 \tag{6}$$

$$\frac{\partial^2 f}{\partial \Phi^2} > 0. \tag{7}$$

It has been verified that $\partial f/\partial\delta E$ changes sign between the in-plane and the out-of-plane regimes. The value of $\partial f/\partial\delta E$

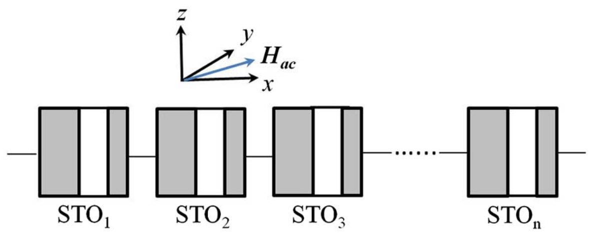

Fig. 7. Schematic illustration of serially connected STOs.

stays negative in the in-plane mode while it stays positive in the out-of-plane mode [17]. Thus the value of $\partial\delta E/\partial\Delta\Phi$ should be negative in the in-plane mode while it should be positive in the out-of-plane mode. It can be observed from Fig. 5 that for $0^\circ \leq \beta < 90^\circ$, the preferred phase shift is 0°; for $90^\circ < \beta \leq 180^\circ$, the preferred phase shift is 180°; and for $\beta = 90^\circ$, the possible preferred phase shift is 90°. These analytical results agree well with our simulation results in Fig. 4(a).

For the out-of-plane mode in Fig. 6, the phase shifts at A' (180°), B' (210°), C' (240°), D' (270°), E' (300°), F' (330°), and G' (360°) are rejected since they do not satisfy the stability criterion, i.e., the condition that $\partial\delta E/\partial\Delta\Phi$ must be positive. The preferred phase shifts are therefore located at points A (0°), B (30°), C (60°), D (90°), E (120°), F (150°), and G (180°) for $\beta = 180^\circ$, $\beta = 150^\circ$, $\beta = 120^\circ$, $\beta = 90^\circ$, $\beta = 60^\circ$, $\beta = 30^\circ$, and $\beta = 0^\circ$, respectively. This tendency also perfectly agrees with our simulation results in Fig. 4(a), and explains why the phase shift can be linearly tuned using an external microwave field as shown in Fig. 4(d).

III. Extension to Multiple STOs

Our approach can be readily extended to multiple STOs. In this configuration (Fig. 7), each individual oscillator is tuned to a preferred phase with respect to the applied microwave field to achieve the synchronization of the entire system. By continuously varying the spatial direction of the applied microwave field, it is possible to vary the I-V phase relation in the STO circuit. By locking the single STO to certain phase shift with external field, the synchronization efficiency and locking range of the serially connected STOs can be improved, thus enhancing the output power. This system will be further investigated.

IV. Conclusion

We report on the preferred phase shift $\Delta\Phi_0$ between an STO and a microwave field H_{ac} where the H_{ac} frequency is the same as the STO intrinsic frequency. It is found both numerically and analytically that a linear tuning relation exists between the microwave field and the STO.

Acknowledgment

This work was supported in part by the Seed Funding Program for Basic Research and Small Project Funding Program from The University of Hong Kong, ITF Tier 3 funding (ITS/112/12), by RGC-GRF under Grant HKU 704911P, and by University Grants Committee of Hong Kong under Contract AoE/P-04/08).

References

[1] J. C. Slonczewski, "Current-driven excitation of magnetic multilayers," *J. Magn. Magn. Mater.*, vol. 159, pp. L1–L7, 1996.
[2] L. Berger, "Emission of spin waves by a magnetic multilayer traversed by a current," *Phys. Rev. B*, vol. 54, pp. 9353–9358, 1996.
[3] J. A. Katine, F. J. Albert, R. A. Buhrman, E. B. Myers, and D. C. Ralph, "Current-driven magnetization reversal and spin-wave excitations in Co /Cu /Co pillars," *Phys. Rev. Lett.*, vol. 84, pp. 3149–3152, 2000.
[4] J. Grollier, V. Cros, A. Hamzic, J. M. George, H. Jaffres, A. Fert, G. Faini, J. B. Youssef, and H. Legall, "Spin-polarized current induced switching in Co/Cu/Co pillars," *Appl. Phys. Lett.*, vol. 78, pp. 3663–3665, 2001.
[5] M. R. Pufall, W. H. Rippard, S. Kaka, T. J. Silva, and S. E. Russek, "Frequency modulation of spin-transfer oscillators," *Appl. Phys. Lett.*, vol. 86, pp. 082506–3, 2005.
[6] Z. Li and S. Zhang, "Thermally assisted magnetization reversal in the presence of a spin-transfer torque," *Phys. Rev. B*, vol. 69, p. 134416, 2004.
[7] G. D. Fuchs, J. A. Katine, S. I. Kiselev, D. Mauri, K. S. Wooley, D. C. Ralph, and R. A. Buhrman, "Spin torque, tunnel-current spin polarization, and magnetoresistance in MgO magnetic tunnel junctions," *Phys. Rev. Lett.*, vol. 96, p. 186603, 2006.
[8] S. I. Kiselev, J. C. Sankey, I. N. Krivorotov, N. C. Emley, M. Rinkoski, C. Perez, R. A. Buhrman, and D. C. Ralph, "Current-induced nanomagnet dynamics for magnetic fields perpendicular to the sample plane," *Phys. Rev. Lett.*, vol. 93, p. 036601, 2004.
[9] J. Grollier, V. Cros, and A. Fert, "Synchronization of spin-transfer oscillators driven by stimulated microwave currents," *Phys. Rev. B*, vol. 73, p. 060409, 2006.
[10] J. Persson, Y. Zhou, and J. Akerman, "Phase-locked spin torque oscillators: Impact of device variability and time delay," *J. Appl. Phys.*, vol. 101, pp. 09A503–3, 2007.
[11] Y. Zhou, J. Persson, and J. Akerman, "Intrinsic phase shift between a spin torque oscillator and an alternating current," *J. Appl. Phys.*, vol. 101, p. 09A510, 2007.
[12] S. E. Russek, S. Kaka, W. H. Rippard, M. R. Pufall, and T. J. Silva, "Finite-temperature modeling of nanoscale spin-transfer oscillators," *Phys. Rev. B*, vol. 71, p. 104425, 2005.
[13] Z. Li and S. Zhang, "Magnetization dynamics with a spin-transfer torque," *Phys. Rev. B*, vol. 68, p. 024404, 2003.
[14] J. Xiao, A. Zangwill, and M. D. Stiles, "Macrospin models of spin transfer dynamics," *Phys. Rev. B*, vol. 72, p. 014446, 2005.
[15] D. Houssameddine, U. Ebels, B. Delaet, B. Rodmacq, I. Firastrau, F. Ponthenier, M. Brunet, C. Thirion, J. P. Michel, L. Prejbeanu-Buda, M. C. Cyrille, O. Redon, and B. Dieny, "Spin-torque oscillator using a perpendicular polarizer and a planar free layer," *Nat. Mater.*, vol. 6, pp. 447–453, 2007.
[16] S. Kaka, M. R. Pufall, W. H. Rippard, T. J. Silva, S. E. Russek, and J. A. Katine, "Mutual phase-locking of microwave spin torque nano-oscillators," *Nature*, vol. 437, pp. 389–392, 2005.
[17] Y. Zhou, J. Persson, S. Bonetti, and J. Akerman, "Tunable intrinsic phase of a spin torque oscillator," *Appl. Phys. Lett.*, vol. 92, pp. 092505–3, 2008.
[18] A. Slavin and V. Tiberkevich, "Nonlinear auto-oscillator theory of microwave generation by spin-polarized current," *IEEE Trans. Magn.*, vol. 45, no. 4, pp. 1875–1918, Apr. 2009.
[19] G. Bertotti, C. Serpico, I. D. Mayergoyz, A. Magni, M. d'Aquino, and R. Bonin, "Magnetization switching and microwave oscillations in nanomagnets driven by spin-polarized currents," *Phys. Rev. Lett.*, vol. 94, p. 127206, 2005.
[20] Z. Li, J. He, and S. Zhang, "Stability of precessional states induced by spin-current," *Phys. Rev. B*, vol. 72, p. 212411, 2005.